



# Low CO<sub>2</sub> evasion rate from the mangrove-surrounding waters of the Sundarbans

Anirban Akhand · Abhra Chanda · Kenta Watanabe · Sourav Das ·  
Tatsuki Tokoro · Kunal Chakraborty · Sugata Hazra · Tomohiro Kuwae

Received: 25 August 2020 / Accepted: 17 February 2021 / Published online: 14 March 2021  
© The Author(s) 2021

**Abstract** Globally, water bodies adjacent to mangroves are considered significant sources of atmospheric CO<sub>2</sub>. We directly measured the partial pressure of CO<sub>2</sub> in water [*p*CO<sub>2</sub>(water)] and related biogeochemical parameters with high temporal resolution, covering both diel and tidal cycles, in the mangrove-surrounding waters around the northern Bay of Bengal during the post-monsoon season. Mean *p*CO<sub>2</sub>(water) was marginally oversaturated in two creeks (470 ± 162 μatm, mean ± SD) and

undersaturated in the adjoining estuarine stations (387 ± 58 μatm) compared to atmospheric *p*CO<sub>2</sub>, and was considerably lower than the global average. We further estimated the *p*CO<sub>2</sub>(water) and buffering capacity of all possible sources of the mangrove-surrounding waters and concluded that their character as a CO<sub>2</sub> sink or weak source is due to the predominance of marine water from the Bay of Bengal with low *p*CO<sub>2</sub> and high buffering capacity. Marine water with high buffering capacity suppresses the effect of *p*CO<sub>2</sub> increase within the mangrove system and lowers the CO<sub>2</sub> evasion even in creek stations. The δ<sup>13</sup>C of dissolved inorganic carbon (DIC) in the mangrove-surrounding waters indicated that the DIC sources were a mixture of mangrove plants, pore-water, and groundwater, in addition to marine water. Finally, we showed that the CO<sub>2</sub> evasion rate from the estuaries of the Sundarbans is much lower than the recently estimated world average. Our results demonstrate that mangrove areas having such low emissions should be considered when up-scaling the global mangrove carbon budget from regional observations.

Responsible Editor: James Sickman

**Supplementary Information** The online version contains supplementary material available at <https://doi.org/10.1007/s10533-021-00769-9>.

A. Akhand (✉) · K. Watanabe · T. Tokoro · T. Kuwae  
Coastal and Estuarine Environment Research Group, Port  
and Airport Research Institute, Yokosuka,  
Kanagawa, Japan  
e-mail: anirban.akhand@gmail.com

A. Chanda · S. Das · S. Hazra  
School of Oceanographic Studies, Jadavpur University,  
Kolkata, West Bengal, India

T. Tokoro  
Center for Global Environmental Research (CGER),  
National Institute for Environmental Studies, Tsukuba,  
Japan

K. Chakraborty  
Indian National Center for Ocean Information Services,  
Ministry of Earth Sciences, Hyderabad, India

**Keywords** Air–water CO<sub>2</sub> flux · Mangrove-surrounding waters · Estuary · *p*CO<sub>2</sub>(water) · Low CO<sub>2</sub> emission

## Introduction

The carbon stocks within several coastal ecosystems (e.g. mangroves, tidal marshes and seagrass beds), collectively referred to as “blue carbon”, have drawn attention in the context of global climate change (Donato et al. 2011; McLeod et al. 2011; Pendleton et al. 2012), and initiatives to characterize the functioning and long-term future of these blue-carbon ecosystems have also begun (Macreadie et al. 2019). These ecosystems are known to be carbon sinks; however, mangroves deserve special mention owing to their large soil organic carbon pool and for being a center for active deposition of both autochthonous and allochthonous organic matter (Breithaupt et al. 2012; Sanders et al. 2016a, 2016b).

Mangroves, despite covering only 0.1% of the Earth’s total land area (Jennerjahn and Ittekkot 2002), are one of the most productive ecosystems in the world, with high carbon-sequestration potential. The carbon (C) stock in mangroves per unit area (956 Mg-C ha<sup>-1</sup>) is much higher than that in other carbon-rich ecosystems such as salt marshes (593 Mg-C ha<sup>-1</sup>), seagrass beds (142 Mg-C ha<sup>-1</sup>), peatland (408 Mg-C ha<sup>-1</sup>), or even rain forests (241 Mg-C ha<sup>-1</sup>) (Alongi 2014; Donato et al. 2011; Twilley et al. 1992).

Although mangrove ecosystems as a whole are net sinks for atmospheric CO<sub>2</sub>, the waters adjacent to mangroves (as well as the associated sediments) emit substantial amounts of CO<sub>2</sub> because they have high organic carbon loading, which is mainly attributed to mangrove biomass, terrestrial detritus, the microphytobenthos, and phytoplankton (Borges et al. 2005, 2018; Borges and Abril 2011; Bouillon and Boschker 2006; Kristensen et al. 2008; Lekphet et al. 2005). In contrast to processes in other forests, tidal flow allows mangroves to exchange both inorganic and organic solutes and particulates with adjacent water bodies (Adame and Lovelock 2011). Several studies have attributed the high CO<sub>2</sub> emissions from mangrove-surrounding waters to the mixing of surface water with pore-water through tidal pumping, which leads to enrichment of the partial pressure of CO<sub>2</sub> in water [*p*CO<sub>2</sub>(water)] and dissolved inorganic carbon (DIC), as well as to metabolic activity in sediments (Bouillon et al. 2007b; Gleeson et al. 2013; Li et al. 2009; Maher et al. 2013; Robinson et al. 2007; Santos et al. 2012; Sippo et al. 2016).

The mineralization of dissolved and particulate organic carbon (DOC and POC, respectively) leads to additional DIC in water bodies adjacent to mangroves (Gattuso et al. 1998; Maher et al. 2013, 2015). The mineralization of organic carbon in mangrove sediments is facilitated through several pathways such as sulfate reduction, iron reduction, and aerobic respiration (Borges et al. 2003; Kristensen and Alongi 2006; Krumins et al. 2013). The diagenetic processes change the balance of exported DIC and total alkalinity (TAlk) from mangroves, which promotes carbonate buffering in the water bodies adjacent to mangroves (Sippo et al. 2016; Joesoef et al. 2017; Maher et al. 2018).

Although the mangrove-surrounding waters (or “mangrove water” or other similar terms) usually act as a source of CO<sub>2</sub>, there are still uncertainties with respect to the global budget of these emissions. Recent measurements in mangrove-surrounding waters showed negative fluxes in some regions and during certain times of the year (Akhand et al. 2013b, 2016; Biswas et al. 2004). In this regard, Reiman and Xu (2019) reported significant underestimation of *p*CO<sub>2</sub>(water) and the air–water CO<sub>2</sub> flux due to the use of a single daily *p*CO<sub>2</sub>(water) value, compared to the diurnal dataset. Rosentreter et al. (2018) emphasized the importance of the temporal resolution of sampling, which can lead to considerable uncertainty. They argued that data acquisition at hourly or greater intervals often misses the tidal maxima and minima, and deducing the mean CO<sub>2</sub> flux from such data might lead to under- or overestimation of fluxes.

The Sundarbans is the world’s largest mangrove forest and has a wide variety of mangrove flora and associated fauna. The Sundarbans mangroves encompass a complex network of channels, creeks and large estuaries. In the last decade, the air–water CO<sub>2</sub> flux has been well studied in the Indian section of the Sundarbans (hereafter, the Indian Sundarbans) in terms of spatial variability (Akhand et al. 2013b, 2016; Dutta et al. 2019) and seasonal variability (Akhand et al. 2016; Biswas et al. 2004). Hence, in this study we do not emphasize these two aspects. Rather, we focus on a particular site previously reported as being a sink or reduced source of CO<sub>2</sub> during the post-monsoon season (Akhand et al. 2016; Biswas et al. 2004) in order to carry out a thorough and comprehensive investigation into the reasons for its being such a sink or weak source in that season.

The hydrology of the Indian Sundarbans is characterized mainly by marine water from the Bay of Bengal (BoB) and to some extent by monsoonal runoff (Cole and Vaidyaraman 1966; Mitra et al. 2009; Sarkar et al. 2004). At present, all rivers in the Indian Sundarbans, except for the Hooghly and its distributary the Muriganga, have lost their direct connections with the main flow of the River Ganga because of siltation in their upper reaches. However, these disconnected rivers receive reduced amounts of riverine freshwater from the Hooghly River through a large number of waterways such as the Hatania-Doania Canal (Ray et al. 2018a).

A unique quality of the BoB is that, despite being part of the open ocean, it has low salinity (Rao and Sivakumar 2003; Prasad 2004; Pant et al. 2015). The main reason for this low salinity is that several large perennial rivers (such as the Ganges, Brahmaputra, Meghna, Mahanadi, and others) discharge into the BoB (Sandeep et al. 2018). The BoB has low  $p\text{CO}_2$  and is considered to be a sink for  $\text{CO}_2$  (Akhand et al. 2013a; Goyet et al. 1999; Kumar et al. 1996). Hence, the tidally driven estuaries of the Indian Sundarbans are affected more by the low- $p\text{CO}_2$  water (nearly equal to or below atmospheric equilibrium) of the BoB than by high- $p\text{CO}_2$  riverine freshwater.

We hypothesized that despite being mangrove-surrounding waters, the  $\text{CO}_2$  sink or weak source character of the Indian Sundarbans is mainly caused by the predominance of water with low- $p\text{CO}_2$  and high-buffering-capacity from the BoB, with higher TAlk than DIC (Goyet et al. 1999; Sabine et al. 2002). To examine this hypothesis, we obtained high-temporal-resolution data for  $p\text{CO}_2(\text{water})$  and other related biogeochemical parameters. In addition, we measured TAlk and DIC along with stable isotopic signatures of DIC to quantify and identify their sources in the surface water. Finally, we compared the estimated fluxes, considering the annual evasion rate over the entire estuary, with global average data. We used the Matla Estuary for comparison, as this estuary flows through the central part of the Indian Sundarbans as well as for a long distance covering almost the entire north–south extent. Moreover, the estuaries of the Sundarbans have been exhaustively studied in the recent past from the perspective of air–water  $\text{CO}_2$  flux (Biswas et al. 2004; Akhand et al. 2013b, 2016; Dutta et al. 2019) as discussed previously. Our objectives were to reduce the uncertainty of flux estimation by

direct and continuous measurement of  $p\text{CO}_2(\text{water})$  in order to confirm the previously observed low  $p\text{CO}_2(\text{water})$  of earlier studies and identify plausible reasons behind such low  $p\text{CO}_2(\text{water})$ .

## Materials and methods

### Study area

The Sundarbans is situated in the lower stretch of the Ganges–Brahmaputra–Meghna (GBM) Delta, extending into both India (40%) and Bangladesh (60%) and facing the BoB to the south. The present study was carried out in the Indian Sundarbans, which comprises an area of 10,200 km<sup>2</sup> out of which 4200 km<sup>2</sup> is demarcated as reserve forest (Ray et al. 2015). Sampling was conducted at six stations in a small north–south section of the estuary approximately 9 km long (width varying between 0.70 and 0.85 km) to the west of Dhanchi Island, and in two tributary creeks ( $\approx 20$  m wide) on the adjoining island (Fig. 1). For details about the study area see Supplementary Material S1. Dhanchi Island covers an area of about 33 km<sup>2</sup>, and its southern tip ends at the BoB. To the east of the island flows the Thankuran Estuary (7 km wide).

### Sample collection

We collected samples at a single station in each of two creeks (hereafter referred to as stations C1 and C2) on the western side of Dhanchi Island, and at six subtidal locations in the adjoining estuary (hereafter referred to as E1, E2, E3, E4, E5 and E6) (Fig. 1). The estuarine stations covered the north-to-south stretch of Dhanchi Island. The abbreviations “C” and “E” stand for “creek” and “estuary”, respectively. Creek stations are more influenced by dense mangrove vegetation than estuarine stations.

Surface  $p\text{CO}_2(\text{water})$ , salinity, water temperature, dissolved oxygen, and chlorophyll-*a* were monitored with sensors (for details see section [Analytical Protocol](#)). Data for a 24-h diurnal cycle for all of these parameters were acquired at 1-min intervals at each of the eight stations between 27 January and 6 February 2018. Surface water samples were collected at two peak low and high tides; i.e. four times from each station during a complete tidal and diurnal cycle for

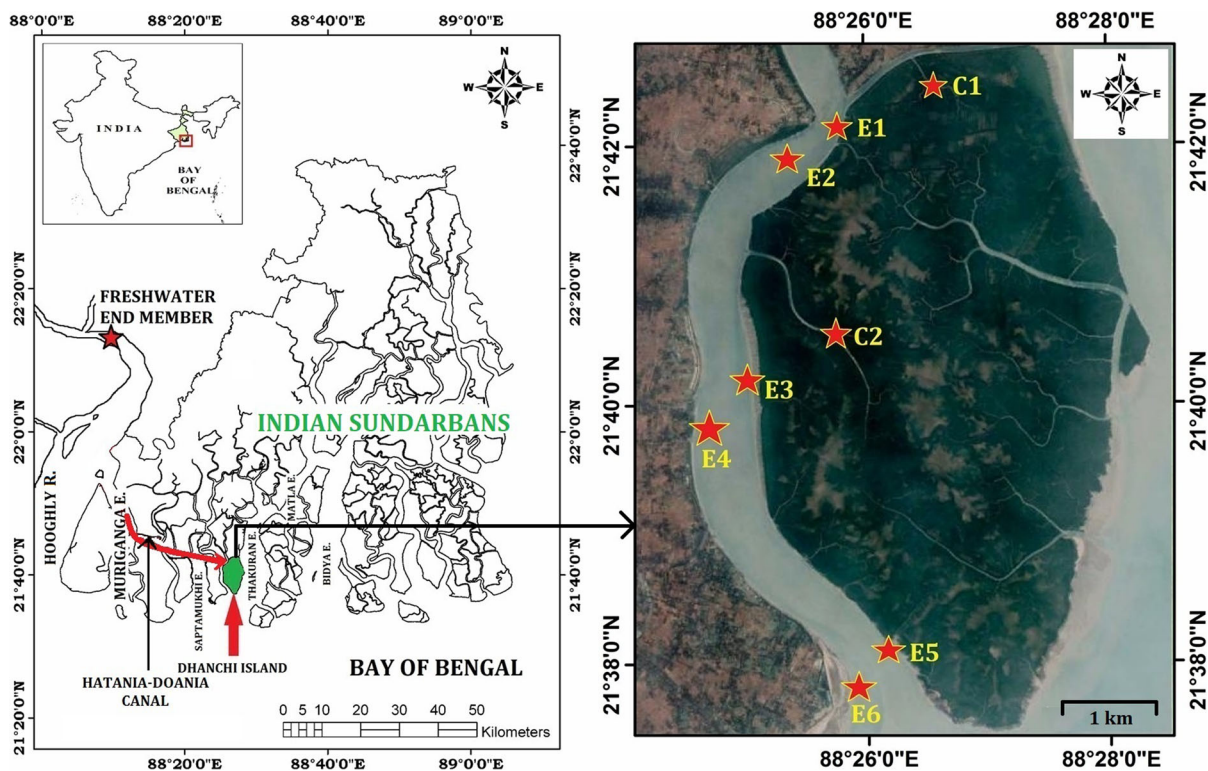


**Fig. 1** Maps of the study area and of Dhanchi Island, located in the Indian Sundarbans. The red stars denote the two creek sampling stations (C1 and C2) and the six estuarine stations (E1, E2, E3, E4, E5 and E6), along with the sampling stations for the riverine freshwater end-member (RFWEM). The red

curved arrow indicates the general pathway of riverine freshwater input to the study area through the Hatania-Doania Canal, which connects the Indian Sundarbans with the Hooghly River (Ray et al. 2018a). (Color figure online)

the analyses of the parameters TALK, DIC, nutrients ( $\text{PO}_4^{3-}$  and  $\text{SiO}_3^{2-}$ ), and  $\delta^{13}\text{C}_{\text{DIC}}$ . In addition, surface water samples were collected from a station named Diamond Harbor (salinity 0.39, measured with the same salinity sensor used for diurnal sampling described later in section Analytical Protocol), which served as the riverine freshwater end-member. The samples were preserved as described in the next paragraph and sent to the laboratory for analysis.

Samples for TALK and DIC were collected into 250-mL Duran bottles (SCHOTT AG, Mainz, Germany), filtered through glass-fiber filters (GF/F; Whatman, Maidstone, Kent, UK) and poisoned with mercuric chloride (200  $\mu\text{L}$  saturated aqueous solution per bottle) to prevent changes in TALK and DIC due to biological activity. Samples for nutrients analyses were collected for input parameters of  $\text{CO}_2\text{SYS}$  software (Lewis and Wallace 1998). The samples were filtered through 0.2- $\mu\text{m}$  polytetrafluoroethylene filters (DISMIC-25HP; Advantec, Durham, NC,

USA) into acid-washed 50-mL polyethylene bottles and frozen at  $-20\text{ }^\circ\text{C}$  until analysis.

#### Analytical protocol

TALK and DIC concentrations were determined using a batch-sample analyzer (ATT-05; Kimoto Electric Co., Ltd., Osaka, Japan) implementing the Gran Plot method (Dickson et al. 2007). The accuracy of TALK and DIC was estimated to be  $\pm 1\ \mu\text{mol kg}^{-1}$  water and  $\pm 2\ \mu\text{mol kg}^{-1}$  water, respectively by triplicate measurements of the certified reference material (CRM) for TALK and DIC (Kanso Company Ltd., Osaka, Japan).

The  $p\text{CO}_2(\text{water})$  was measured with a  $\text{CO}_2$  analyzer (non-dispersive infrared sensor) through an equilibrator system ( $\text{CO}_2\text{-09}$ , Kimoto Electric Co., Ltd.) (Kayanne et al. 1995; Tokoro et al. 2014) using a gas-permeable membrane (Saito et al. 1995). The instrument was calibrated every day at the beginning

of the measurements using certified reference gases [pure N<sub>2</sub> gas (0 ppm) and span gas (600 ppm CO<sub>2</sub> gas with a N<sub>2</sub> base; Chemtron Science Laboratories, Mumbai, India)]. The estimated accuracy and precision of the *p*CO<sub>2</sub> analyzer were ± 5 μatm and ± 2 μatm, respectively, which was in parity with the previous works (Saito et al. 1995, 1999; Kayanne et al. 2005) where the same *p*CO<sub>2</sub> measurement system was used.

Stable isotope signatures (δ<sup>13</sup>C<sub>DIC</sub>) were measured with an isotope-ratio mass spectrometer (Delta Plus Advantage; Thermo Electron, Bremen, Germany) coupled with an elemental analyzer (Flash EA 1112; Thermo Electron) following the method of Miyajima et al. (1995). Stable isotope ratios are expressed in δ notation as the deviation from standards in parts per thousand (‰) according to the following equation:

$$\delta^{13}C_{DIC} = [R_{sample}/R_{standard} - 1] \times 10^3 \quad (1)$$

where *R* is <sup>13</sup>C/<sup>12</sup>C. Vienna Pee Dee Belemnite (VPDB) was used as the isotope standard for carbon. The analytical precision of the Delta Plus Advantage mass-spectrometer system, based on the standard deviation of the internal reference replicates, was < 0.2‰ for δ<sup>13</sup>C<sub>DIC</sub>.

Salinity and temperature were measured with a CT-sensor (INFINITY-CT; JFE Advantech CO., Ltd, Nishinomiya, Japan). Dissolved oxygen (DO) concentration was measured at hourly intervals with a portable DO meter (FiveGo Series; Mettler Toledo, Giessen, Germany). Chlorophyll-*a* concentration (Chl-*a*) and turbidity were measured in situ with a fluorometer (COMPACT-CLW, JFE Advantech CO., Ltd). The Chl-*a* fluorescence sensor was adjusted in a uranine solution by the manufacturer to yield a constant calibration factor. We have corrected the Chl-*a* data using the regression line between sensor data and 12 spectrophotometrically measured Chl-*a* data collected during sampling. Chl-*a* was measured following standard spectrophotometric procedures using Shimadzu UV–Visible 1600 double-beam spectrophotometer (Parsons et al. 1992). Nutrients concentrations (PO<sub>4</sub><sup>3-</sup> and SiO<sub>3</sub><sup>2-</sup>) in sample filtrates were measured using an Auto Analyzer (QuAAtro; BL TEC K. K., Osaka, Japan; for nutrient data, see Table S1, Supplementary Material).

### Estimation of air–water CO<sub>2</sub> flux

The air–water CO<sub>2</sub> flux (*F*<sub>CO<sub>2</sub></sub>, μmol CO<sub>2</sub> m<sup>-2</sup> h<sup>-1</sup>) was determined by the following equation:

$$F_{CO_2} = k \times K_0 \times \Delta pCO_2 \quad (2)$$

where *k* is the gas transfer velocity (cm h<sup>-1</sup>), *K*<sub>0</sub> denotes the solubility coefficient of CO<sub>2</sub> (mol m<sup>-3</sup> atm<sup>-1</sup>), and Δ*p*CO<sub>2</sub> denotes the difference in fugacity (≈ partial pressure) of CO<sub>2</sub> between water and air [*p*CO<sub>2</sub>(water) – *p*CO<sub>2</sub>(air)]. *K*<sub>0</sub> is computed based on the equation given by Weiss (1974). The *p*CO<sub>2</sub>(air) was considered to be 408 μatm, i.e. the global mean *p*CO<sub>2</sub>(air) observed during the study period (<https://www.co2.earth/historical-co2-datasets>). The mole fraction of CO<sub>2</sub> was converted to partial pressure of CO<sub>2</sub> in air [*p*CO<sub>2</sub>(air)] by using the virial equation of state (Weiss 1974). A positive *F*<sub>CO<sub>2</sub></sub> value indicates CO<sub>2</sub> efflux from the water to the atmosphere and vice versa. The parameter *k* was calculated by using three different empirical gas transfer velocity models based on wind speed: Liss and Merlivat (1986) (LM86), Raymond et al. (2000) (R00) and Ho et al. (2011) (H11). These formulae were selected for the present study because the estuarine channels in the Indian Sundarbans are very wide and there is no hindrance to the free-flowing wind, which makes the wind velocity the most important component regulating the CO<sub>2</sub> fluxes. The equations for the gas transfer velocity calculations are given below:

$$k = 0.17 \times U_{10} \times \left(\frac{660}{S_c}\right)^{0.5} \quad \text{for } U_{10} \leq 3.6 \text{ m s}^{-1} \quad (LM86) \quad (3a)$$

$$k = (2.85 \times U_{10} - 9.65) \times \left(\frac{660}{S_c}\right)^{0.5} \quad \text{for } 3.6 < U_{10} < 13 \text{ m s}^{-1} \quad (LM86) \quad (3b)$$

$$k = 2.78 \times U_{10}^{0.46} \times \left(\frac{660}{S_c}\right)^{0.5} \quad (R00) \quad (4)$$

$$k = (a + 0.266 \times U_{10}^2) \times \left(\frac{660}{S_c}\right)^{0.5} \quad (H11) \quad (5)$$

where  $U_{10}$  is the wind speed at 10-m height and  $a$  is a constant accounting for gas transfer from bottom-shear-driven turbulence (assumed to be zero in the present study area, in accordance with Ho et al. [2011] and their study in the wide Hudson Bay, USA).  $Sc$  is the Schmidt number of  $CO_2$  as given by Jähne et al. (1987). Only Eq. (3a) was used to compute the gas transfer velocity according to *LM86*, because the mean wind speed was always  $< 3.6 \text{ m s}^{-1}$  during the present study. Wind speed data were acquired by using a handheld anemometer (AM 4201; Lutron Inc., Singapore) and corrected for the 10-m measurement height (Kondo 2000).

### Data analysis

The Hooghly River is the main “artery” (Ray et al. 2018a) and only possible source of riverine freshwater to the Indian Sundarbans. For this reason, the near-zero salinity region of the Hooghly River has been widely used in previous works (Dutta et al. 2019; Ray and Shahraki 2016; Ray et al. 2015, 2018a) as the freshwater end-member for the Indian Sundarbans. In accordance with these previous studies, we defined the observed salinity at the Diamond Harbor station (salinity approx. 0) as a proxy for the riverine freshwater end-member. Figure 1 includes a schematic showing the pathway of riverine freshwater input to the study area through the Hatania-Doania Canal, which connects the Indian Sundarbans with the Hooghly River (Ray et al. 2018a).

To characterize the pathway of mineralization of organic matter in this study, we normalized both TALK and DIC with respect to salinity. We analyzed the stoichiometric relationship (the slope) between salinity-normalized TALK (nTALK) and salinity-normalized DIC (nDIC). DIC was normalized according to the following equation (Friis et al. 2003):

$$nDIC = \left[ \left\{ \frac{DIC_{meas} - DIC_{S=0}}{S_{meas}} \right\} \times S_{mean} \right] \quad (6)$$

where  $DIC_{meas}$  is the measured DIC,  $DIC_{S=0}$  is the DIC of the riverine freshwater end-member (i.e. where salinity = 0),  $S_{meas}$  is the measured salinity, and  $S_{mean}$  is the mean salinity, which is used for normalization (25.0 for this study). TALK was also normalized using the same equation, replacing  $DIC_{meas}$  and  $DIC_{S=0}$  with  $TALK_{meas}$  and  $TALK_{S=0}$ , respectively.

Excess DIC for the creek and estuarine stations was calculated from the difference between the “in situ DIC” and the expected DIC in water when  $pCO_2(\text{water})$  is equal to  $pCO_2(\text{air})$  (Abril et al. 2000). The latter was determined by using *CO2SYS* software with the in situ salinity, temperature, measured alkalinity and an atmospheric  $pCO_2$  of  $408 \mu\text{atm}$  as input parameters.

pH was estimated from the measured TALK and DIC values ( $n = 31$ ) using *CO2SYS* software (version 2.5) (Lewis and Wallace 1998). The uncertainty in pH estimation was 0.012 (estimated from the accuracy of the input parameters, TALK and DIC, stated in section *Analytical Protocol*, by using the error computation tool of the *CO2SYS* software).

We estimated the  $pCO_2(\text{water})$  and Revelle factor of the sampled waters and all possible sources of the estuarine water—namely pore-water, groundwater, the riverine freshwater end-member, and offshore water of the northern BoB—by using *CO2SYS* software (Lewis and Wallace 1998). For the riverine freshwater end-member, we used the measured TALK and DIC of the present study and data from previous studies (Akhand et al. 2016; Dutta et al. 2019) to calculate the Revelle factor. For groundwater, the  $pCO_2(\text{water})$  and Revelle factor were calculated by using measured TALK and DIC (Akhand et al., unpublished data; see details of the sample collection in Table S2, Supplementary Material). We used the pore-water pH data of Mandal et al. (2009) and pore-water DIC data of Dutta et al. (2019) (from samples collected from various sites in the Indian Sundarbans, depth reported as 30 cm below the water table) as input parameters in *CO2SYS* to compute the  $pCO_2(\text{water})$  and Revelle factor of pore-water. For the northern BoB, we used the measured pH and TALK data of Akhand et al. (2012) and Sarma et al. (2012) [we used only the data from the station nearest to the Indian Sundarbans from Sarma et al. (2012)]. For waters farther offshore in the BoB (almost to latitude  $10^\circ\text{N}$ ) we used the TALK and DIC data of Goyet et al. (1999) to compute the Revelle factor. Unlike for the other possible sources, we could estimate only a single value of the Revelle factor and the  $pCO_2(\text{water})$  for pore-water and water from offshore in the BoB. We believe that as the data for pore-water is close to that of ground water and data from the far offshore BoB is close to the data from the northern BoB, these representative single data will not hamper any interpretation of the present study.

Oxygen saturation was calculated according to the solubility equation given by Benson and Krause (1984). Apparent oxygen utilization (AOU) was calculated according to the formula,  $AOU = C_{\text{obs}} - C_{\text{sat}}$ , where  $C_{\text{obs}}$  is the observed DO concentration and  $C_{\text{sat}}$  is the oxygen concentration at saturation.

Statistical analyses were done using SPSS software version 16.0 (SPSS Inc., Chicago, USA). We checked for normality of the biogeochemical parameters—namely salinity, water temperature, DO,  $p\text{CO}_2(\text{water})$ , pH, TALK, DIC, TALK/DIC,  $\delta^{13}\text{C}_{\text{DIC}}$  and Chl-*a*—by applying the Shapiro–Wilk test. All of these parameters exhibited non-normal distributions. In order to test the significance of differences in these parameters between the creek and estuarine stations, we applied the non-parametric Mann–Whitney *U* test (also known as the Wilcoxon rank sum test).

## Results

### Physicochemical setting

Salinity and water temperature were significantly higher in the creeks than in the estuary (salinity,  $p < 0.001$ ; water temperature,  $p < 0.001$ ; Mann–Whitney *U* test) but varied within very narrow ranges (Table 1). DO concentrations were significantly higher in the estuary than in the creeks ( $p < 0.001$ , Table 1). Chl-*a* concentrations were significantly higher in the creeks than in the estuary ( $p < 0.001$ , Table 1).

### Carbonate-chemistry parameters

There were no significant differences in mean TALK and DIC between the creeks and estuary, but some creek samples had high values during ebb tide (TALK,  $2732 \mu\text{mol kg}^{-1}$ ; DIC,  $2683 \mu\text{mol kg}^{-1}$ ) (Fig. 2a, b). No significant difference was found in TALK/DIC ( $p > 0.05$ ) (Fig. 2c).  $p\text{CO}_2(\text{water})$  and  $\delta^{13}\text{C}_{\text{DIC}}$  were significantly different between creeks and estuary ( $p < 0.001$ ); the mean  $p\text{CO}_2(\text{water})$  was oversaturated in the creeks ( $470 \pm 162 \mu\text{atm}$ , mean  $\pm$  SD), and undersaturated in the estuary ( $387 \pm 58 \mu\text{atm}$ ) with respect to  $p\text{CO}_2(\text{air})$  ( $408 \mu\text{atm}$ ) (Fig. 3 and Table 1), whereas, the mean pH was slightly lower in the creeks ( $7.91 \pm 0.16$ ) than in the estuary ( $7.96 \pm 0.06$ ); however, the difference was not significant ( $p > 0.05$ , Table 1).  $\delta^{13}\text{C}_{\text{DIC}}$  varied over a wide range,

from  $-1.5\text{‰}$  to  $-7.6\text{‰}$  with a mean of  $-3.4\text{‰} \pm 1.9\text{‰}$  and  $-1.9\text{‰} \pm 0.2\text{‰}$  in the creeks and estuary, respectively (Fig. 2d). Both Chl-*a* (Fig. 4a, b) and turbidity (Fig. 4c, d) showed significant positive correlations with  $p\text{CO}_2(\text{water})$  ( $p < 0.001$ ).

The Revelle factor varied over a wide range among the possible sources of the mangrove-surrounding waters in the estuary (Table 2). The mean Revelle factors at the creek and estuarine stations were  $12.8 \pm 2.1$  (range, 11.2–17.9) and  $12.4 \pm 1.4$  (11.5–16.3), respectively. The Revelle factor of the riverine freshwater end-member was 26.7. The estimated Revelle factors of the northern BoB and the waters farther offshore in the BoB (almost to latitude  $10^\circ\text{N}$ ) were 7.5–8.1 and 8.9, respectively, whereas those of pore-water and groundwater were 17.6 and 14.9, respectively.

DIC showed significant negative correlations with  $\delta^{13}\text{C}_{\text{DIC}}$  both in the creeks ( $r = -0.990$ ,  $p < 0.001$ ) and the estuary ( $r = -0.980$ ,  $p < 0.001$ ) (Fig. 5a). There were significant negative correlations between TALK/DIC and excess DIC both in the creeks ( $r = -0.995$ ;  $p < 0.001$ ) and the estuary ( $r = -0.980$ ;  $p < 0.001$ ) (Fig. 5b). nDIC and nTALK were significantly correlated in the creeks ( $r = 0.995$ ;  $p < 0.001$ ) and in the estuary ( $r = 0.992$ ;  $p < 0.001$ ), with slopes of 0.84 and 0.81, respectively (Fig. 5c). There was no significant correlation between AOU and excess DIC ( $p < 0.001$ , Fig. 5d).

### Air–water $\text{CO}_2$ flux

Both the creek and estuarine stations exhibited diel and tidal variation in air–water  $\text{CO}_2$  fluxes, and acted as both sinks and sources of atmospheric  $\text{CO}_2$  at different times over the diel cycle (Fig. 5). The creeks acted as net sources of  $\text{CO}_2$  with a mean flux of  $13 \pm 34 \mu\text{mol m}^{-2} \text{h}^{-1}$ ,  $107 \pm 284 \mu\text{mol m}^{-2} \text{h}^{-1}$  and  $69 \pm 180 \mu\text{mol m}^{-2} \text{h}^{-1}$  according to Eqs. (3a), (4), and (5), respectively. In contrast, the estuary acted as a net sink for  $\text{CO}_2$  with a mean flux of  $-4 \pm 12 \mu\text{mol m}^{-2} \text{h}^{-1}$ ,  $-37 \pm 95 \mu\text{mol m}^{-2} \text{h}^{-1}$  and  $-23 \pm 64 \mu\text{mol m}^{-2} \text{h}^{-1}$  according to Eqs. (3a), (4), and (5), respectively.

**Table 1** Mean  $\pm$  standard deviation and range (in parentheses) of all high-temporal-resolution physicochemical and carbonate-chemistry parameters measured with sensors at creek (C) and estuarine (E) stations, and the estimated pH

Station	C1	C2	C (Average of C1 and C2)	E1	E2	E3	E4	E5	E6	E (Average of E1 to E6)
Tidal phase	4th Day after NT	1st day after ST		5th day after NT	6th day after NT	2nd day after ST	ST	3rd day after ST	4th Day after ST	
Parameter										
Water temperature (°C)	20.94 $\pm$ 0.46 (20.27–22.52) <i>n</i> = 1440	21.41 $\pm$ 0.75 (19.44–22.52) <i>n</i> = 1440	21.18 $\pm$ 0.66 (19.44–22.52) <i>n</i> = 2880	21.13 $\pm$ 0.41 (20.41–22.35) <i>n</i> = 1440	21.32 $\pm$ 0.19 (21.09–22.01) <i>n</i> = 1440	21.96 $\pm$ 0.19 (21.50–22.44) <i>n</i> = 1440	21.62 $\pm$ 0.19 (21.37–21.90) <i>n</i> = 1440	22.29 $\pm$ 0.23 (21.99–22.83) <i>n</i> = 1440	22.42 $\pm$ 0.15 (22.22–22.83) <i>n</i> = 1440	21.78 $\pm$ 0.53 (20.41–22.83) <i>n</i> = 8640
Salinity	24.83 $\pm$ 0.16 (24.22–25.12) <i>n</i> = 1440	25.92 $\pm$ 0.46 (25.01–27.62) <i>n</i> = 1440	25.37 $\pm$ 0.65 (24.22–27.62) <i>n</i> = 2880	25.01 $\pm$ 0.07 (24.89–25.21) <i>n</i> = 1440	25.24 $\pm$ 0.08 (25.07–25.59) <i>n</i> = 1440	25.83 $\pm$ 0.09 (25.60–26.04) <i>n</i> = 1440	25.57 $\pm$ 0.12 (25.27–25.79) <i>n</i> = 1440	26.05 $\pm$ 0.15 (25.80–26.34) <i>n</i> = 1440	26.05 $\pm$ 0.16 (25.86–26.37) <i>n</i> = 1440	25.62 $\pm$ 0.41 (24.89–26.37) <i>n</i> = 8640
Dissolved oxygen (mg L <sup>-1</sup> )	5.1 $\pm$ 0.2 (4.8–5.4) <i>n</i> = 24	5.0 $\pm$ 0.2 (4.7–5.3) <i>n</i> = 24	5.1 $\pm$ 0.2 (4.7–5.4) <i>n</i> = 48	5.4 $\pm$ 0.2 (5.1–5.7) <i>n</i> = 24	5.9 $\pm$ 0.2 (5.5–6.2) <i>n</i> = 24	5.4 $\pm$ 0.2 (5.0–5.9) <i>n</i> = 24	6.0 $\pm$ 0.2 (5.6–6.2) <i>n</i> = 24	5.6 $\pm$ 0.2 (5.3–6.0) <i>n</i> = 24	5.9 $\pm$ 0.1 (5.7–6.3) <i>n</i> = 24	5.7 $\pm$ 0.3 (5.0–6.4) <i>n</i> = 144
Chlorophyll- <i>a</i> (mg m <sup>-3</sup> )	1.83 $\pm$ 0.48 (0.33–6.46) <i>n</i> = 1419	1.79 $\pm$ 0.61 (0.84–5.00) <i>n</i> = 1205	1.71 $\pm$ 0.90 (0.33–6.46) <i>n</i> = 2624	1.15 $\pm$ 0.31 (0.52–4.61) <i>n</i> = 1394	1.14 $\pm$ 0.23 (0.33–3.10) <i>n</i> = 1382	NA	1.40 $\pm$ 0.23 (0.79–3.98) <i>n</i> = 1393	1.23 $\pm$ 0.38 (0.63–3.23) <i>n</i> = 1398	1.09 $\pm$ 0.25 (0.58–2.14) <i>n</i> = 1034	1.33 $\pm$ 0.57 (0.33–6.45) <i>n</i> = 6601
pCO <sub>2</sub> (water) (µatm)	417 $\pm$ 92 (315–709) <i>n</i> = 1440	523 $\pm$ 197 (369–1204) <i>n</i> = 1440	470 $\pm$ 162 (315–1204) <i>n</i> = 2880	356 $\pm$ 53 (311–610) <i>n</i> = 1440	344 $\pm$ 13 (320–390) <i>n</i> = 1440	425 $\pm$ 39 (368–576) <i>n</i> = 1440	355 $\pm$ 14 (331–410) <i>n</i> = 1440	397 $\pm$ 14 (380–450) <i>n</i> = 1440	443 $\pm$ 83 (375–636) <i>n</i> = 1440	387 $\pm$ 58 (311–636) <i>n</i> = 8640
pH	7.98 $\pm$ 0.05 (7.93–8.03) <i>n</i> = 4	7.85 $\pm$ 0.21 (7.54–7.97) <i>n</i> = 4	7.91 $\pm$ 0.16 (7.54–8.03) <i>n</i> = 8	7.89 $\pm$ 0.13 (7.70–8.00) <i>n</i> = 4	7.99 $\pm$ 0.02 (7.96–8.00) <i>n</i> = 4	7.96 $\pm$ 0.01 (7.95–7.98) <i>n</i> = 4	7.99 $\pm$ 0.01 (7.99–7.98) <i>n</i> = 4	7.97 $\pm$ 0.01 (7.96–7.98) <i>n</i> = 4	7.95 $\pm$ 0.04 (7.90–7.98) <i>n</i> = 3	7.96 $\pm$ 0.06 (7.70–8.00) <i>n</i> = 23

For tidal and diurnal variability of these variables see Fig. 3 and Supplementary Figure S1  
ST Spring Tide, NT Neap Tide, NA data not available

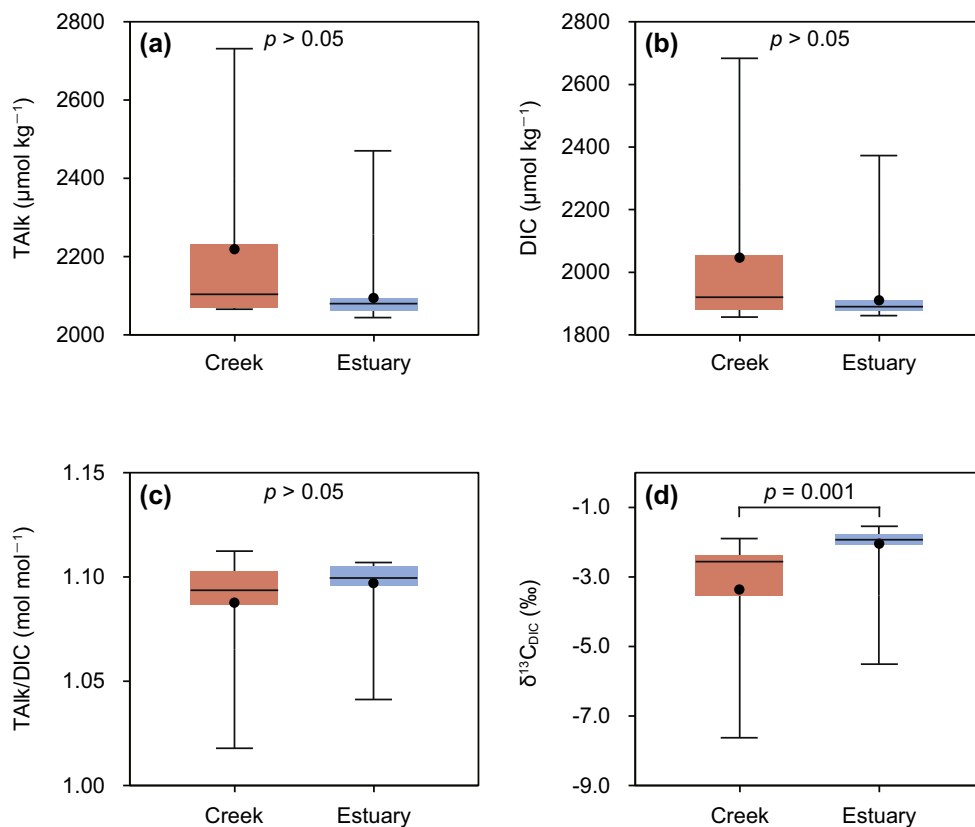


**Fig. 2** Box-and-whisker plots of **a** TALK, **b** DIC, **c** TALK/DIC, and **d**  $\delta^{13}\text{C}_{\text{DIC}}$  at the creek and estuarine stations. The box-and-whisker plots show the median (centerline), the mean (closed

circle), the 25th and 75th percentiles (lower and upper edges of the box, respectively) and the minimum and maximum values (whiskers). (Color figure online)

## Discussion

### Sinks and low effluxes of $\text{CO}_2$ in comparison with the global average

Our results show that the estuary clearly acted as a net  $\text{CO}_2$  sink and the mangrove creeks acted as a weak source of  $\text{CO}_2$ . The uncertainty of the estimated  $p\text{CO}_2(\text{water})$  and air–water  $\text{CO}_2$  flux was lower compared to previous studies in the Sundarbans because of the higher temporal resolution (cf. Rosentreter et al. 2018) and direct estimation of  $p\text{CO}_2(\text{water})$  (cf. David et al. 2018). We compared the  $p\text{CO}_2(\text{water})$  and air–water  $\text{CO}_2$  flux with values from other studies around the world (Table 3), focusing on the recent studies that used high-temporal-resolution direct measurements of  $p\text{CO}_2(\text{water})$  or air–water  $\text{CO}_2$  flux. It is evident that no previous study of mangrove-surrounding waters reported such a mean low  $p\text{CO}_2(\text{water})$  as

that in the present study, although several previous studies reported values in the lower range of  $p\text{CO}_2(\text{water})$  from the mangrove creeks that were equal to or lower than the atmospheric  $\text{CO}_2$  concentration (Call et al. 2015; Sippo et al. 2016; Rosentreter et al. 2018). The low  $p\text{CO}_2(\text{water})$  observed in the present study indicates that sometimes the mangrove-surrounding waters act as a sink or weak source of atmospheric  $\text{CO}_2$ . Nevertheless, our high-temporal-resolution and direct  $p\text{CO}_2$  measurements can reduce the uncertainty in the data for the air–water  $\text{CO}_2$  flux of mangrove-surrounding waters showing high spatio-temporal variability.

The air–water  $\text{CO}_2$  flux data for the mangrove-surrounding waters obtained by the present study and previous studies in the Sundarbans are markedly lower than the recently reported global average. Even the annual mean  $\text{CO}_2$  flux for the entire Matla Estuary (approximately  $6.3 \pm 0.9 \text{ mmol m}^{-2} \text{ d}^{-1}$ ; Akhand et al.

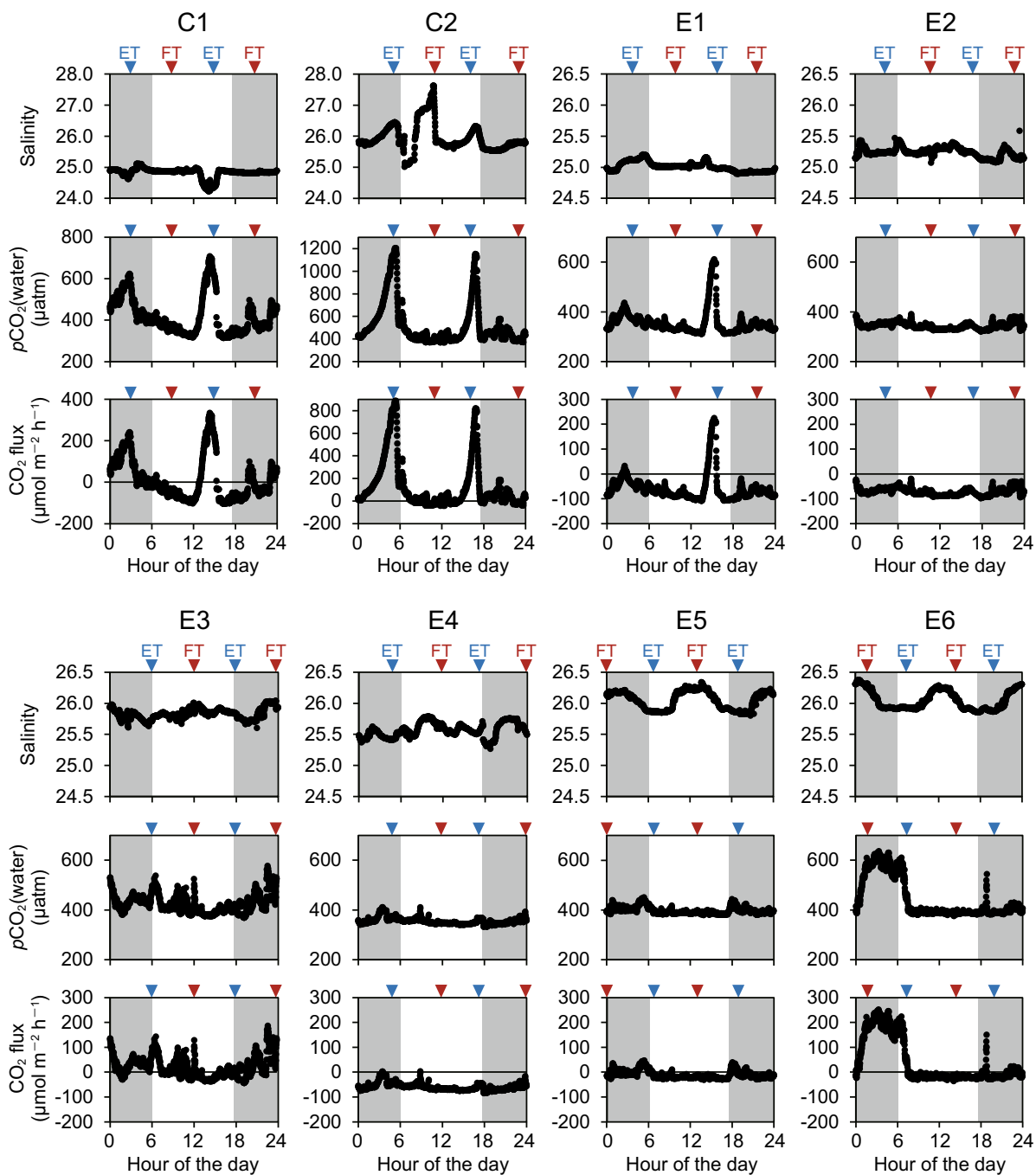


**Fig. 3** Time-series plots of diel variation of salinity,  $p\text{CO}_2(\text{water})$  ( $\mu\text{atm}$ ), and  $\text{CO}_2$  flux [ $\mu\text{mol m}^{-2} \text{h}^{-1}$ ]; according to the wind parameterization of Ho et al. (2011) at the two creek stations (C1 and C2) and the six estuarine stations (E1, E2, E3,

E4, E5 and E6). FT, flood tide; ET, ebb tide. The shaded regions show the night-time portion of the diel cycle. (Color figure online)

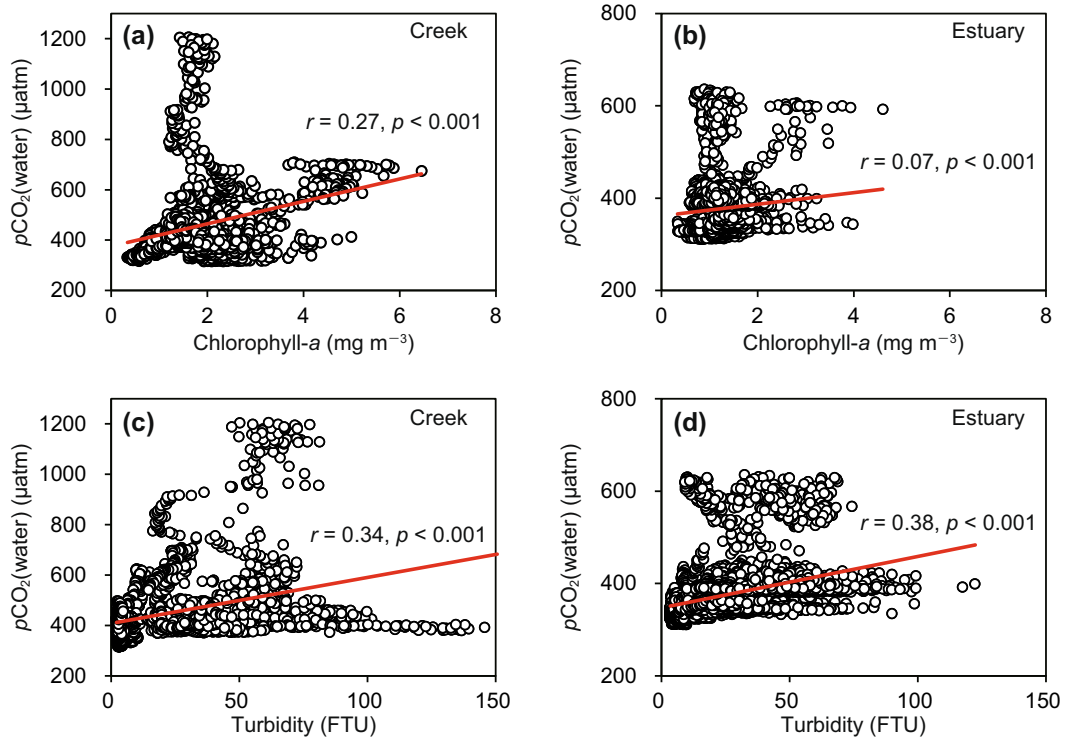


**Fig. 4** Relationship between chlorophyll-*a* concentration and  $p\text{CO}_2(\text{water})$  in **a** the creek stations and **b** the estuarine stations. Relationship between turbidity (FTU, Formazin Turbidity Unit)

and  $p\text{CO}_2(\text{water})$  in **c** the creek stations and **d** the estuarine stations. Red straight lines indicate regression lines. (Color figure online)

**Table 2** Revelle factors and  $p\text{CO}_2(\text{water})$  values at the study site and in potential sources of mangrove-surrounding waters in the Indian Sundarbans

Water types	Revelle factor	$p\text{CO}_2(\text{water})$ ( $\mu\text{atm}$ )	Source of estimate
<b>Potential Sources</b>			
Riverine freshwater end-member	26.7–33.6	1421–4678	Present study Akhand et al. (2016) Dutta et al. (2019)
Pore-water of Sundarbans	17.6	$\approx 5423$	Mandal et al. (2009) Dutta et al. (2019)
Groundwater of Sundarbans	14.9–18.4	506–1219	Akhand et al. (unpublished data)
Northern Bay of Bengal	7.5–8.1	149–299	Sarma et al. (2012) Akhand et al. (2012)
Bay of Bengal ( $\approx 10^\circ\text{N}$ latitude)	8.9	$\approx 340$	Goyet et al. (1999)
<b>Study sites</b>			
Creek stations	11.0–14.1	315–1204	Present study
Estuarine stations	10.9–12.5	311–636	Present study

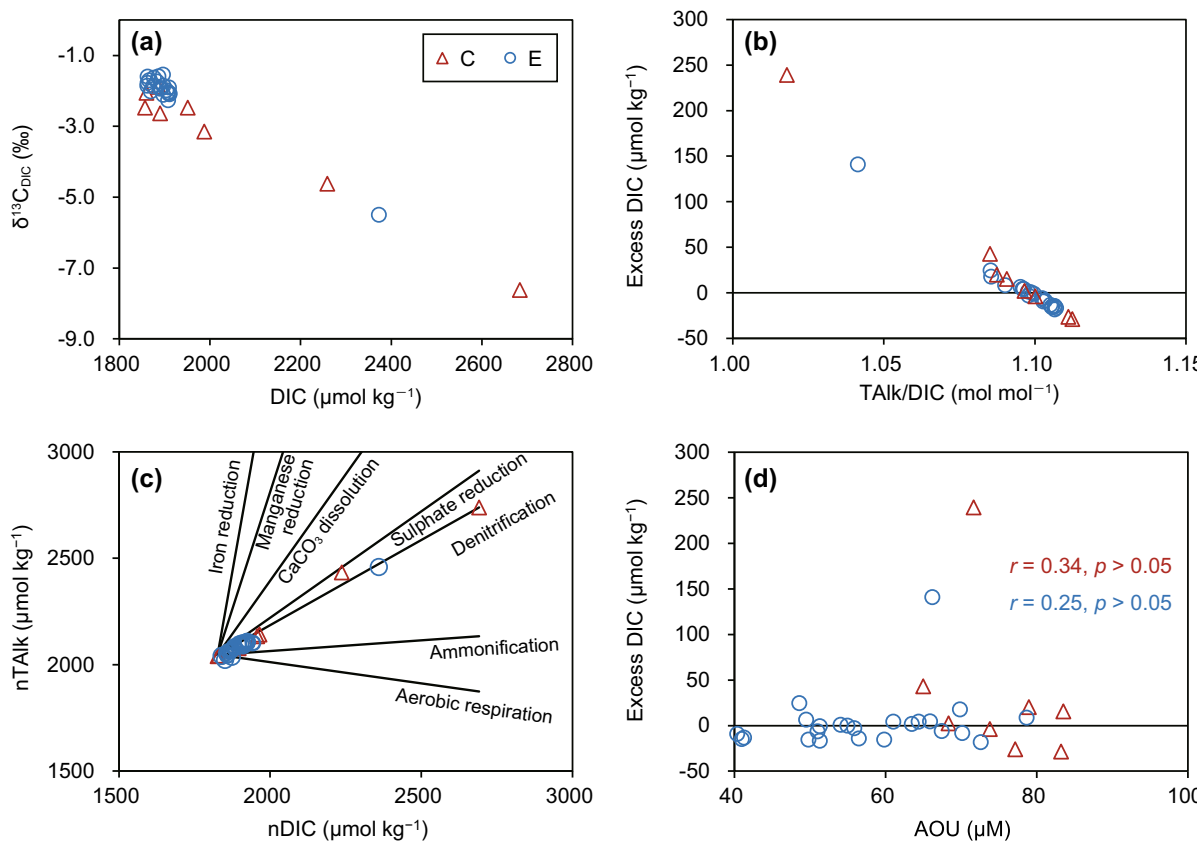


**Fig. 5** **a** Relationship between DIC and  $\delta^{13}\text{C}_{\text{DIC}}$ . **b** Relationship between TALK/DIC and excess DIC. **c** Relationship between salinity-normalized TALK (nTALK) and salinity-normalized DIC (nDIC). The lines correspond to the theoretical covariation of

2016) is much less than the world average for emissions from mangrove-associated water ( $56.8 \pm 8.9 \text{ mmol m}^{-2} \text{ d}^{-1}$ ; Rosentreter et al. 2018) (Fig. 6).

#### Predominance of marine water and low $p\text{CO}_2$

The waters around mangroves usually exhibit significant diel and tidal variability in terms of both  $p\text{CO}_2(\text{water})$  and air–water  $\text{CO}_2$  flux, with higher  $p\text{CO}_2(\text{water})$  values during low tides and vice versa (Zablocki et al. 2011). However, the continuous high-temporal-resolution measurements in this study showed that these changes in  $p\text{CO}_2(\text{water})$  with the tide occurred only at the creek stations (Fig. 3) and not at the estuarine stations, except for station E1. The high  $p\text{CO}_2(\text{water})$  during low tide is generally attributed to  $p\text{CO}_2$ -rich pore-water as well as

nTALK and nDIC for various metabolic pathways. The colored circles and triangles indicate data from the present study. **d** Relationship between AOU and excess DIC. C, creek stations; E, estuarine stations. (Color figure online)

groundwater, and the low  $p\text{CO}_2(\text{water})$  during flood tide results from the dilution of mangrove-derived water (Akhand et al. 2016; Call et al. 2015; Maher et al. 2013). The absence of  $p\text{CO}_2(\text{water})$  maxima during low tide at our estuarine stations suggests that the pore-water, which seems to have a prominent effect in the creeks, did not play a significant role in regulating the diel variation of  $p\text{CO}_2(\text{water})$  at these estuarine stations. The most plausible reason behind this observation might be that the higher marine water volume in the estuarine stations and higher water residence time in the creek stations exceed the effect of pore-water in the estuarine stations even during the low tide period.

The Revelle factor is the ratio of the relative change of  $p\text{CO}_2(\text{water})$  to the corresponding relative change of DIC in marine water; thus, it reflects the carbonate

**Table 3**  $p\text{CO}_2(\text{water})$  and air–water  $\text{CO}_2$  fluxes observed in this study (mean  $\pm$  standard deviation), and in recent studies that directly measured  $p\text{CO}_2(\text{water})$  and/or air–water  $\text{CO}_2$  flux of mangrove-surrounding waters. *LM86*, *R00*, and *H11* indicate

that the gas transfer velocities in the present study were calculated according to Eq. (3a) (Liss and Merlivat 1986), Eq. (4) (Raymond et al. 2000) or Eq. (5) (Ho et al. 2011), respectively

Location	$p\text{CO}_2(\text{water})$ [ $\mu\text{atm}$ ]	$\text{CO}_2$ flux ( $\text{mmol CO}_2 \text{ m}^{-2} \text{ d}^{-1}$ )	Remarks	Authors
North Brazil	592–15,361	$174 \pm 129$	Spring to neap tidal cycle	Call et al. (2019)
Ouemo archipelago, New Caledonia	NA	11–1620	Dec 2016 to Sept 2017 (at 3-week intervals) only during high tides	Jacotot et al. (2018)
Vietnam	660–5000	74–876	24-h cycle in dry and wet seasons	David et al. (2018)
Queensland, Australia	387–13,031	58.7–277.6	Wet and dry seasons	Rosentreter et al. (2018)
Bali, Indonesia	NA	$18.1 \pm 5.8$	55-h time series measurements	Macklin et al. (2019)
Sundarbans, India, creek stations	315–1204	$0.3 \pm 0.8$ ( <i>LM86</i> ) $2.6 \pm 6.8$ ( <i>R00</i> ) $1.6 \pm 4.3$ ( <i>H11</i> )	Two weeks of post-monsoon (dry) season	Present study
Sundarbans, India, estuarine stations	311–636	$-0.1 \pm 0.3$ ( <i>LM86</i> ) $-1.0 \pm 2.3$ ( <i>R00</i> ) $-0.7 \pm 1.7$ ( <i>H11</i> )	Two weeks of post-monsoon (dry) season	Present study

NA data not available

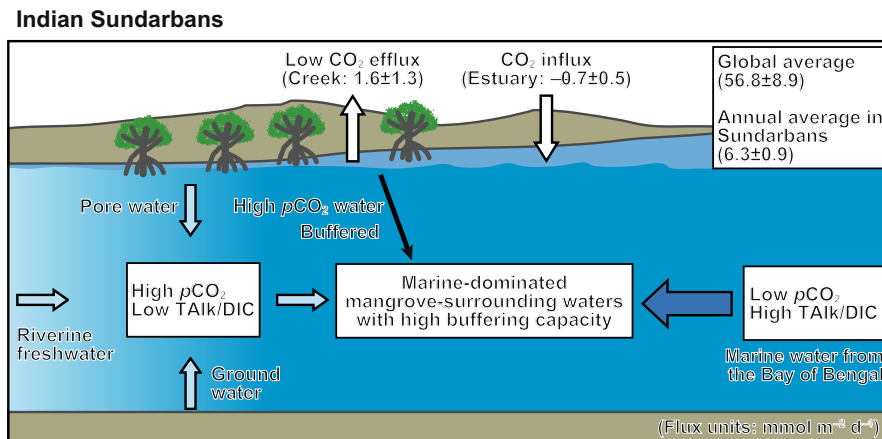


**Fig. 6** Schematic diagram of the underlying mechanism behind the low  $\text{CO}_2$  evasion rate from the mangrove-surrounding waters of the Indian Sundarbans. The mean ( $\pm$  SE, standard error) air–water  $\text{CO}_2$  flux data presented in this study (white arrows) are based on the gas transfer velocity  $k$  ( $\text{cm h}^{-1}$ ) from the

model of Ho et al. (2011) (Eq. 5). The annual mean air–water  $\text{CO}_2$  flux data for the Sundarbans and the global average data are adopted from Akhand et al. (2016) and Rosentreter et al. (2018), respectively. (Color figure online)

buffering capacity of the water mass and is implicitly related to the TAlk/DIC ratio (Egleston et al. 2010). A low Revelle factor can indicate high carbonate buffering capacity and the potential for  $\text{CO}_2$  uptake

(Bates et al. 2012; Sabine et al. 2004). Among the possible sources of water in the mangrove-dominated estuary in this study, the riverine freshwater end-member, groundwater, and pore-water had both

$p\text{CO}_2(\text{water})$  values and Revelle factors higher than the observed values in the creeks and estuary (Table 2). In contrast, the waters from the northern BoB and farther offshore had  $p\text{CO}_2(\text{water})$  and an estimated Revelle factor lower than the waters at the study site (Table 2). These results indicate that the low- $p\text{CO}_2$  waters of the BoB have higher buffering capacity than all of the other possible sources of water in this estuary. Thus, we infer that the low  $p\text{CO}_2(\text{water})$  of the Sundarbans may be due mainly to the predominance of BoB water with low  $p\text{CO}_2(\text{water})$  (Akhand et al. 2012, 2013a; Goyet et al. 1999; Sarma et al. 2012) and high buffering capacity.

Another reason behind the low  $p\text{CO}_2(\text{water})$  of this study site, in addition to the predominance of low- $p\text{CO}_2$  water from the BoB, might be that the Indian Sundarbans receives comparatively less riverine freshwater input than other river-dominated estuaries (Chakrabarti 1998; Mitra et al. 2009). River-dominated estuaries having large riverine freshwater inputs have shown higher  $p\text{CO}_2(\text{water})$  than marine-dominated estuaries having less riverine freshwater inputs (Akhand et al. 2016; Jiang et al. 2008; Maher and Eyre 2012). The rapid export of material because of estuarine geometry and the meso- to macro-tidal nature of this estuary further enhance the low  $p\text{CO}_2(\text{water})$  character. Specifically, Ray et al. (2018a) and references therein have shown that the rapid transport of material from Sundarbans mangroves to the BoB is due to (i) the shorter water residence time, (ii) large tidal amplitudes, and (iii) the funnel-shaped geometry of the estuary, which tends to amplify the tide, in turn facilitating faster material transport.

#### Effects of mangroves on air–water $\text{CO}_2$ flux

The measured TALK and DIC in the present study are in agreement with the reported ranges for TALK and DIC for other mangrove-associated waters that act as net sources of  $\text{CO}_2$  (David et al. 2018; Linto et al. 2014; Ray et al. 2018b; Zablocki et al. 2011) despite the sink and weak source behaviors of the Indian Sundarbans. Some high TALK and DIC values at creek stations during ebb tide suggest that the TALK and DIC were added from the mangrove ecosystem. The significant negative correlation between TALK/DIC and excess DIC in both creeks and estuary suggests that higher TALK/DIC suppressed excess DIC and contributed to

the  $\text{CO}_2$  sink or weak source character (Fig. 5b). Exports of higher TALK-to-DIC ratios from mangroves to coastal waters, with a TALK/DIC ratio of 1.2, led to an overall increase in pH and thus had a buffering effect (Sippo et al. 2016). The TALK/DIC at our sites was  $1.08 \pm 0.06$  ( $\text{mol mol}^{-1}$ ), indicating a relatively high buffering capacity in the mangrove-surrounding waters of the Sundarbans, but it was not markedly higher than that observed in other parts of the world (1.00–1.10; Sippo et al. 2016). Increased pH and under-saturation of  $p\text{CO}_2$  in mangrove-surrounding waters can also occur as a result of the remnant TALK after  $\text{CO}_2$  outgassing and outwelling of mangrove TALK, as discussed by Sippo et al. (2016).

Our results showed that diagenetic processes in this mangrove system reduced TALK/DIC ratios, which increased  $p\text{CO}_2$  in the mangrove-surrounding waters (Fig. 6). The diagenesis of organic carbon in mangroves sediments takes place through several anaerobic pathways that supply TALK and DIC and change the pore-water TALK/DIC (Borges et al. 2003; Bouillon et al. 2007b; Koné and Borges 2008). The relationships between nDIC and nTALK in this study, with slopes of 0.84 (creeks) and 0.81 (estuary) (Fig. 5c), suggest denitrification, as observed in the waters around mangroves in the Mekong Delta, Vietnam (Alongi et al. 2000) and Gaji Bay, Kenya (Bouillon et al. 2007a). Denitrification has previously been reported in the mangrove sediment of the Indian (Das et al. 2013, 2020; Ray et al. 2014) and Bangladesh (Neogi et al. 2016) Sundarbans. Das et al. (2020) reported a mean denitrification rate of  $14.72 \text{ nmol N}_2\text{O-N h}^{-1} (\text{g dry wt})^{-1}$  in the sediments of Lothian Island (Indian Sundarbans). The absence of a significant correlation between AOU and excess DIC (Fig. 5d) suggests that aerobic respiration was not the major diagenetic pathway for organic matter (OM) degradation in the present study. A primary assumption of the method of delineating the diagenetic pathway of OM mineralization using the nDIC:nTALK ratio is that the C, N, and P of the OM follows the Redfield ratio (Krumins et al. 2013). However, the organic matter in the mangrove-surrounding waters might not always match the Redfield ratio, which implies an uncertainty in this stoichiometric analysis. Still, our principal purpose was to understand the nDIC:nTALK ratio from the perspective of the carbonate buffering capacity, rather than determining the exact organic matter mineralization pathway. The

nDIC:nTAlk ratios indicate that the diagenetic pathways at the study site provide a lower buffering capacity than the marine water, and increased excess DIC and  $p\text{CO}_2$  (Fig. 5b and c). Marine water with high buffering capacity suppresses the effect of  $p\text{CO}_2$  increase in the mangrove system and the lowers  $\text{CO}_2$  evasion even in the creek stations (Fig. 5b).

The effect of mangroves on carbonate chemistry in coastal waters is variable depending on the biogeochemical processes in the mangrove systems. We found that the mean pH value at the more marine-influenced estuarine stations was higher than that at the more mangrove-influenced creek stations (Table 1); however, the difference of pH was not found to be significant between creek and estuarine stations ( $p > 0.05$ ). pH values reported in the offshore waters of the BoB (8.13–8.46) were much higher (by 0.1–0.4 units; Akhand et al. 2012, 2013a; Sarma et al. 2012) than the pH values observed in both the creek and the estuarine stations (Table 1). These results also support our suggestion that the low  $p\text{CO}_2(\text{water})$  of the mangrove-surrounding waters can be attributed to the effect of BoB water with low  $p\text{CO}_2$  (Akhand et al. 2012, 2013a; Goyet et al. 1999; Sarma et al. 2012;) and higher buffering capacity rather than to the effect of mangroves.

Biological uptake of DIC is also an important factor in explaining low  $p\text{CO}_2(\text{water})$  as well as the air–water  $\text{CO}_2$  flux. Both buffering capacity and Revelle factor can be affected by biological factor(s) (Hauck and Volker, 2015; Hauck et al. 2015). In the present study, higher mean Chl-*a* concentrations (Table 1 and Supplementary Fig. S1) were associated with  $p\text{CO}_2(\text{water})$  above saturation at the creek stations and vice versa at the estuarine stations (Table 2). However, there was no significant negative relationship between Chl-*a* concentration and  $p\text{CO}_2(\text{water})$  at any of the stations, rather a significant positive correlation was found (Fig. 4a and b). These results indicate that biological control of  $p\text{CO}_2(\text{water})$  was less important than physical mixing in this study. However, the negative excess DIC at several creek stations (Fig. 5b) might be related to higher phytoplankton production, which would contribute to reducing the  $\text{CO}_2$  effluxes. The significant positive correlation between Chl-*a* and  $p\text{CO}_2(\text{water})$ , along with significant positive correlation between turbidity

and  $p\text{CO}_2(\text{water})$  (Fig. 4c and d), indicates that high Chl-*a* with turbidity led to a high organic matter degradation rate and high DIC input as observed in some previous studies (Abril et al. 2000; Fay and McKinley 2017; Tishchenko et al. 2018).

We found a significant negative correlation between DIC and  $\delta^{13}\text{C}_{\text{DIC}}$  (Fig. 5a), with higher DIC values and lower  $\delta^{13}\text{C}_{\text{DIC}}$  values in the creeks than in the estuary (Fig. 2b and d). This suggests that the sources of DIC have lighter  $\delta^{13}\text{C}$  values and were supplied from the mangroves. The most plausible explanation for the DIC sources is therefore a combination of mineralization of mangrove tissue ( $\delta^{13}\text{C}_{\text{TOC}} = -28.08\text{‰}$  to  $-26.31\text{‰}$ ; Ray et al. 2015), POC in the water around mangroves ( $\delta^{13}\text{C}_{\text{POC}} = -23.3\text{‰}$  to  $-22.3\text{‰}$ ; Dutta et al. 2019; Ray et al. 2015), and marine phytoplankton ( $-22.0\text{‰}$  to  $-20.0\text{‰}$ ; Rosentreter et al. 2018). Groundwater DIC and pore-water DIC ( $-18.0\text{‰}$ , pore-water DIC in Sundarbans, Dutta et al. 2019;  $-14.5\text{‰}$  to  $-10.0\text{‰}$ , ground water/pore-water DIC, Maher et al. 2013) are also possible DIC sources. We assumed that air–water  $\text{CO}_2$  fluxes had a negligible effect on isotopic fractionation, as the fluxes were at near-equilibrium. This type of mixed source for DIC has been reported in other mangrove environments (Maher et al. 2017; Rosentreter et al. 2018; Sea et al. 2018). Under such a scenario, the carbon dynamics in the mangrove-surrounding waters cannot be explained solely by mangrove-derived DIC loading, but must also be regulated by other allochthonous sources (Rosentreter et al. 2018).

## Conclusion

The results of this study suggest that mangrove-surrounding waters can act as a sink or a weak source for atmospheric  $\text{CO}_2$ , contrary to most previous studies. There have been previous studies of  $\text{CO}_2$  dynamics in the Sundarbans, but the precision and temporal resolution of the data were too coarse to determine source/sink characteristics. The present study successfully overcame these problems and reduced the uncertainties by analyzing the diel variability of  $p\text{CO}_2(\text{water})$  at eight sites, covering tidal maxima and minima. Our findings further show that the  $\text{CO}_2$  sink or weak source character of the Sundarbans' mangrove-surrounding waters was caused by predominance of the low- $p\text{CO}_2$  and high-

buffering-capacity waters of the BoB. The TALK export from the mangroves also buffers the increase in  $p\text{CO}_2$  owing to the DIC addition. The marine water with high TALK/DIC ratio buffers the effect of  $p\text{CO}_2$  increase in the mangrove systems, lowering  $\text{CO}_2$  evasion in the study site. Finally, we argue that areas with such low emissions should be included when the global mangrove carbon budget is estimated by scaling-up regional observations.

**Acknowledgements** We are grateful for funding this work provided by the Environmental Research and Technology Development Fund (S-14) and the Japan Society for the Promotion of Science (KAKENHI 18H04156 and 19K20500). We are also thankful to National Remote Sensing Centre (Department of Space, Government of India) for partial funding of this work. We thank the West Bengal Forest Department for granting us the necessary permissions. We also thank Ms. N. Umegaki for help with the chemical analyses.

**Authors' contributions** AA, AC, KW, SH, and TK designed the study. AA, AC, and SD did the field work and sample collection. AA, AC, KW, SD, TT, and KC did the chemical and data analyses. AA, AC, KW, SH, and TK wrote the manuscript. All authors read and approved the manuscript.

**Funding** This work was supported by funding through the Environmental Research and Technology Development Fund (S-14) and the Japan Society for the Promotion of Science (KAKENHI 18H04156 and 19K20500). This work was also supported by partial funding of the National Remote Sensing Centre (Department of Space, Government of India).

**Data availability** Dataset is archived in the Zenodo database (<https://doi.org/10.5281/zenodo.4572499>; Akhand et al. 2021\_Biogeochemistry).

**Code availability** Not applicable.

## Declarations

**Conflict of interest** The authors declare that the research was conducted in the absence of any commercial or financial relationships that could be construed as a potential conflict of interest.

**Open Access** This article is licensed under a Creative Commons Attribution 4.0 International License, which permits use, sharing, adaptation, distribution and reproduction in any medium or format, as long as you give appropriate credit to the original author(s) and the source, provide a link to the Creative Commons licence, and indicate if changes were made. The images or other third party material in this article are included in the article's Creative Commons licence, unless indicated otherwise in a credit line to the material. If material is not included in the article's Creative Commons licence and your intended use is not permitted by statutory regulation or exceeds

the permitted use, you will need to obtain permission directly from the copyright holder. To view a copy of this licence, visit <http://creativecommons.org/licenses/by/4.0/>.

## References

- Abril G, Etcheber H, Borges AV, Frankignoulle M (2000) Excess atmospheric carbon dioxide transported by rivers into the Scheldt estuary. *Comptes Rendus de l'Academie des Sciences-Series IIA-Earth Planet. Sci* 330(11):761–768. [https://doi.org/10.1016/S1251-8050\(00\)00231-7](https://doi.org/10.1016/S1251-8050(00)00231-7)
- Adame MF, Lovelock CE (2011) Carbon and nutrient exchange of mangrove forests with the coastal ocean. *Hydrobiologia* 663(1):23–50. <https://doi.org/10.1007/s10750-010-0554-7>
- Akhand A, Chanda A, Dutta S, Hazra S (2012) Air–water carbon dioxide exchange dynamics along the outer estuarine transition zone of Sundarban, northern Bay of Bengal. *India Indian J Geomar Sci* 41(2):111–116
- Akhand A, Chanda A, Dutta S, Manna S, Hazra S, Mitra D, Rao KH, Dadhwal VK (2013a) Characterizing air–sea  $\text{CO}_2$  exchange dynamics during winter in the coastal water off the Hugli-Matla estuarine system in the northern Bay of Bengal. *India J Oceanogr* 69(6):23–50. <https://doi.org/10.1007/s10872-013-0199-z>
- Akhand A, Chanda A, Dutta S, Manna S, Sanyal P, Hazra S, Rao KH, Dadhwal VK (2013b) Dual character of Sundarban estuary as a source and sink of  $\text{CO}_2$  during summer: an investigation of spatial dynamics. *Environ Monit Assess* 185(8):4461–4480. <https://doi.org/10.1007/s10661-012-3042-x>
- Akhand A, Chanda A, Manna S, Das S, Hazra S, Roy R, Choudhury SB, Rao KH, Dadhwal VK, Chakraborty K, Mostofa KMG, Tokoro T, Kuwae T (2016) A comparison of  $\text{CO}_2$  dynamics and air–water fluxes in a river-dominated estuary and a mangrove-dominated marine estuary. *Geophys Res Lett.* <https://doi.org/10.1002/2016GL070716>
- Akhand A, Chanda A, Watanabe K, Das S, Tokoro T, Chakraborty K, Hazra S, Kuwae T (2021) Dataset for the article entitled “Low  $\text{CO}_2$  evasion rate from the mangrove-surrounding waters of the Sundarbans”. Zenodo. <https://doi.org/10.5281/zenodo.4572499>
- Alongi DM (2014) Carbon cycling and storage in mangrove forests. *Annu Rev Mar Sci* 6:195–219. <https://doi.org/10.1146/annurev-marine-010213-135020>
- Alongi DM, Tirendi F, Trott LA, Xuan TT (2000) Benthic decomposition rates and pathways in plantations of the mangrove *Rhizophora apiculata* in the Mekong delta. *Vietnam Mar Ecol Prog Ser* 194:87–101. <https://doi.org/10.3354/meps194087>
- Bates NR, Best MHP, Neely K, Garley R, Dickson AG, Johnson RJ (2012) Detecting anthropogenic carbon dioxide uptake and ocean acidification in the North Atlantic Ocean. *Biogeochemistry* 9(1):2509–2522. <https://doi.org/10.5194/bg-9-2509-2012>
- Benson BB, Krause D Jr (1984) The concentration and isotopic fractionation of oxygen dissolved in freshwater and

- seawater in equilibrium with the atmosphere. *Limnol Oceanogr* 29(3):620–632. <https://doi.org/10.4319/lo.1984.29.3.0620>
- Biswas H, Mukhopadhyay SK, De TK, Sen S, Jana TK (2004) Biogenic controls on the air–water carbon dioxide exchange in the Sundarban mangrove environment, northeast coast of Bay of Bengal. *India Limnol Oceanogr* 49(1):95–101. <https://doi.org/10.4319/lo.2004.49.1.0095>
- Borges AV, Abril G (2011) Carbon Dioxide and Methane Dynamics in Estuaries. In: Wolanski E, McLusky DS (eds) *Treatise on Estuarine and Coastal Science*. Academic Press, Waltham, pp 119–161
- Borges AV, Djenidi S, Lacroix G, Théate J, Delille B, Frankignoulle M (2003) Atmospheric CO<sub>2</sub> flux from mangrove surrounding waters. *Geophys Res Lett*. <https://doi.org/10.1029/2003GL017143>
- Borges AV, Delille B, Frankignoulle M (2005) Budgeting sinks and sources of CO<sub>2</sub> in the coastal ocean: Diversity of ecosystems counts. *Geophys Res Lett*. <https://doi.org/10.1029/2005GL023053>
- Borges AV, Abril G, Bouillon S (2018) Carbon dynamics and CO<sub>2</sub> and CH<sub>4</sub> outgassing in the Mekong delta. *Biogeochemistry* 15(4):1093–1114. <https://doi.org/10.5194/bg-15-1093-2018>
- Bouillon S, Boschker HTS (2006) Bacterial carbon sources in coastal sediments: a cross-system analysis based on stable isotope data of biomarkers. *Biogeochemistry* 3:175–185. <https://doi.org/10.5194/bg-3-175-2006>
- Bouillon S, Dehairs F, Velimirov B, Abril G, Borges AV (2007a) Dynamics of organic and inorganic carbon across contiguous mangrove and seagrass systems (Gazi Bay, Kenya). *J Geophys Res Biogeosci*. <https://doi.org/10.1029/2006JG000325>
- Bouillon S, Middelburg JJ, Dehairs F, Borges AV, Abril G, Flindt MR, Ulomi S, Kristensen E (2007b) Importance of intertidal sediment processes and porewater exchange on the water column biogeochemistry in a pristine mangrove creek (Ras Dege, Tanzania). *Biogeochemistry* 4:311–322. <https://doi.org/10.5194/bg-4-311-2007>
- Breithaupt JL, Smoak JM, Smith TJ III, Sanders CJ, Hoare A (2012) Organic carbon burial rates in mangrove sediments: Strengthening the global budget. *Glob Biogeochem Cycle*. <https://doi.org/10.1029/2012GB004375>
- Call M, Maher DT, Santos IR, Ruiz-Halpern S, Mangion P, Sanders CJ, Erler DV, Oakes JM, Rosentreter J, Murray R, Eyre BD (2015) Spatial and temporal variability of carbon dioxide and methane fluxes over semi-diurnal and spring–neap–spring timescales in a mangrove creek. *Geochim Cosmochim Acta* 150:211–225. <https://doi.org/10.1016/j.gca.2014.11.023>
- Call M, Santos IR, Dittmar T, de Rezende CE, Asp NE, Maher DT (2019) High pore-water derived CO<sub>2</sub> and CH<sub>4</sub> emissions from a macro-tidal mangrove creek in the Amazon region. *Geochim Cosmochim Acta* 247:106–120. <https://doi.org/10.1016/j.gca.2018.12.029>
- Chakrabarti PS (1998) Changing courses of Ganga, Ganga-Padma river system, West Bengal, India—RS data usage in user orientation, river behavior and control. *J River Res Institute* 25:19–40
- Cole, C. V., Vaidyaraman, P. P. (1966). “Salinity distribution and effect of freshwater flows in the Hooghly River” in *Proceedings of the 10th Conference on Coastal Engineering*, Tokyo, Japan (American Society of Civil Engineers, New York), September 1966, 1312–1434.
- Das S, Ganguly D, Mukherjee A, Chakraborty S, De TK (2020) Exploration of N<sub>2</sub> fixation and denitrification processes in the Sundarban mangrove ecosystem, India. *Indian Journal of Geo Marine Sciences* 49(05):740–747
- Das S, Ganguly D, Maiti TK, Mukherjee A, Jana TK, De TK (2013) A depth wise diversity of free living N<sub>2</sub> fixing and nitrifying bacteria and its seasonal variation with nitrogen containing nutrients in the mangrove sediments of Sundarban, WB. *India Open J Mar Sci* 3(02):112–119. <https://doi.org/10.4236/ojms.2013.32012>
- David F, Meziane T, Tran-Thi NT, Van VT, Thanh-Nho N, Taillardat P, Marchand C (2018) Carbon biogeochemistry and CO<sub>2</sub> emissions in a human impacted and mangrove dominated tropical estuary (Can Gio, Vietnam). *Biogeochemistry* 138:261–275. <https://doi.org/10.1007/s10533-018-0444-z>
- Dickson AG, Sabine CL, Christian JR (2007) *Guide to Best Practices for Ocean CO<sub>2</sub> Measurements*. PICES Special Publication, North Pacific Marine Science Organization, Canada
- Donato DC, Kauffman JB, Murdiyarto D, Kurnianto S, Stidham M, Kanninen M (2011) Mangroves among the most carbon-rich forests in the tropics. *Nat Geosci* 4(5):293–297. <https://doi.org/10.1038/NGEO1123>
- Dutta MK, Kumar S, Mukherjee R, Sanyal P, Mukhopadhyay SK (2019) The post-monsoon carbon biogeochemistry of the Hooghly-Sundarbans estuarine system under different levels of anthropogenic impacts. *Biogeochemistry* 16(2):289–307. <https://doi.org/10.5194/bg-16-289-2019>
- Egleston ES, Sabine CL, Morel FM (2010) Revelle revisited: Buffer factors that quantify the response of ocean chemistry to changes in DIC and alkalinity. *Glob Biogeochem Cycles*. <https://doi.org/10.1029/2008GB003407>
- Fay AR, McKinley GA (2017) Correlations of surface ocean pCO<sub>2</sub> to satellite chlorophyll on monthly to interannual timescales. *Glob Biogeochem Cycles*. <https://doi.org/10.1002/2016GB005563>
- Friis K, Körtzinger A, Wallace DW (2003) The salinity normalization of marine inorganic carbon chemistry data. *Geophys Res Lett*. <https://doi.org/10.1029/2002GL015898>
- Gattuso JP, Frankignoulle M, Wollast R (1998) Carbon and carbonate metabolism in coastal aquatic ecosystems. *Annu Rev Ecol Syst* 29(1):405–434. <https://doi.org/10.1146/annurev.ecolsys.29.1.405>
- Gleeson J, Santos IR, Maher DT, Golsby-Smith L (2013) Groundwater–surface water exchange in a mangrove tidal creek: evidence from natural geochemical tracers and implications for nutrient budgets. *Mar Chem* 156:27–37. <https://doi.org/10.1016/j.marchem.2013.02.001>
- Goyet C, Coataoan C, Eiseheid G, Amaoka T, Okuda K, Healy R, Tsunogai S (1999) Spatial variation of total CO<sub>2</sub> and total alkalinity in the northern Indian Ocean: A novel approach for the quantification of anthropogenic CO<sub>2</sub> in seawater. *J Mar Res* 57(1):135–163. <https://doi.org/10.1357/002224099765038599>
- Hauck J, Völker C (2015) Rising atmospheric CO<sub>2</sub> leads to large impact of biology on Southern Ocean CO<sub>2</sub> uptake via

- changes of the Revelle factor. *Geophys Res Lett.* <https://doi.org/10.1002/2015GL063070>
- Hauck J, Völker C, Wolf-Gladrow DA, Laufkötter C, Vogt M, Aumont O, Bopp L, Buitenhuis ET, Doney SC, Dunne J, Gruber N (2015) On the Southern Ocean CO<sub>2</sub> uptake and the role of the biological carbon pump in the 21st century. *Glob Biogeochem Cycles.* <https://doi.org/10.1002/2015GB005140>
- Ho DT, Schlosser P, Orton PM (2011) On factors controlling air-water gas exchange in a large tidal river. *Estuaries Coast* 34(6):1103–1116. <https://doi.org/10.1007/s12237-011-9396-4>
- Jacotot A, Marchand C, Allenbach M (2018) Tidal variability of CO<sub>2</sub> and CH<sub>4</sub> emissions from the water column within a Rhizophora mangrove forest (New Caledonia). *Sci Tot Environ.* <https://doi.org/10.1016/j.scitotenv.2018.03.006>
- Jähne B, Heinz G, Dietrich W (1987) Measurement of the diffusion coefficients of sparingly soluble gases in water. *J Geophys Res Oceans.* <https://doi.org/10.1029/JC092iC10p10767>
- Jennerjahn TC, Ittekkot V (2002) Relevance of mangroves for the production and deposition of organic matter along tropical continental margins. *Naturwissenschaften* 89(1):23–30. <https://doi.org/10.1007/s00114-001-0283-x>
- Jiang LQ, Cai WJ, Wang Y (2008) A comparative study of carbon dioxide degassing in river- and marine-dominated estuaries. *Limnol Oceanogr* 53(6):2603–2615. <https://doi.org/10.4319/lo.2008.53.6.2603>
- Joesoef A, Kirchman DL, Sommerfield CK, Wei-Jun C (2017) Seasonal variability of the inorganic carbon system in a large coastal plain estuary. *Biogeochemistry.* <https://doi.org/10.5194/bg-14-4949-2017>
- Kayanne H, Hata H, Kudo S, Yamano H, Watanabe A, Ikeda Y, Nozaki K, Kato K, Negishi A, Saito H (2005) Seasonal and bleaching-induced changes in coral reef metabolism and CO<sub>2</sub> flux. *Glob Biogeochem Cycle.* <https://doi.org/10.1029/2004GB002400>
- Kayanne H, Suzuki A, Saito H (1995) Diurnal changes in the partial pressure of carbon dioxide in coral reef water. *Science* 269(5221):214–216. <https://doi.org/10.1126/science.269.5221.214>
- Kondo J (2000) *Atmosphere Science near the Ground Surface.* University of Tokyo Press, Tokyo, Japan
- Koné YM, Borges AV (2008) Dissolved inorganic carbon dynamics in the waters surrounding forested mangroves of the Ca Mau Province (Vietnam). *Estuar Coast Shelf Sci* 77(3):409–421. <https://doi.org/10.1016/j.ecss.2007.10.001>
- Kristensen E, Alongi DM (2006) Control by fiddler crabs (*Uca vocans*) and plant roots (*Avicennia marina*) on carbon, iron, and sulfur biogeochemistry in mangrove sediment. *Limnol Oceanogr* 51(4):1557–1571. <https://doi.org/10.4319/lo.2006.51.4.1557>
- Kristensen E, Flindt MR, Ulomi S, Borges AV, Abril G, Bouillon S (2008) Emission of CO<sub>2</sub> and CH<sub>4</sub> to the atmosphere by sediments and open waters in two Tanzanian mangrove forests. *Mar Ecol Prog Ser* 370:53–67. <https://doi.org/10.3354/meps07642>
- Krumins V, Gehlen M, Arndt S, Cappellen PV, Regnier P (2013) Dissolved inorganic carbon and alkalinity fluxes from coastal marine sediments: Model estimates for different shelf environments and sensitivity to global change. *Biogeochemistry* 10(1):371–398. <https://doi.org/10.5194/bg-10-371-2013>
- Kumar MD, Naqvi SWA, George MD, Jayakumar DA (1996) A sink for atmospheric carbon dioxide in the northeast Indian Ocean. *J Geophys Res: Oceans.* <https://doi.org/10.1029/96JC01452>
- Lekphet S, Nitisoravut S, Adsavakulchai S (2005) Estimating methane emissions from mangrove area in Ranong Province Thailand Songklanakar. *J Sci Tech* 27(1):153–163
- Lewis E, Wallace DWR (1998) Program developed for CO<sub>2</sub> system calculations, ORNL/CDIAC – 105. Department of Energy, Oak Ridge, Tennessee, U.S.A, Carbon Dioxide Information Analysis Center, Oak Ridge National Laboratory, U.S
- Li X, Hu BX, Burnett WC, Santos IR, Chanton JP (2009) Submarine groundwater discharge driven by tidal pumping in a heterogeneous aquifer. *Groundwater* 47(4):558–568. <https://doi.org/10.1111/j.1745-6584.2009.00563.x>
- Linto N, Barnes J, Ramachandran R, Divia J, Ramachandran P, Upstill-Goddard RC (2014) Carbon dioxide and methane emissions from mangrove-associated waters of the Andaman Islands. *Bay of Bengal Estuar Coast* 37(2):381–398. <https://doi.org/10.1007/s12237-013-9674-4>
- Liss PS, Merlivat L (1986) Air-Sea Gas Exchange Rates: Introduction and Synthesis. In: Buat-Ménard P (ed) *The Role of Air-Sea Exchange in Geochemical Cycling* NATO ASI Series Series C Mathematical and Physical Sciences. Springer, Dordrecht, p 185
- Macklin PA, Suryaputra IGNA, Maher DT, Murdiyarto D, Santos IR (2019) Drivers of CO<sub>2</sub> along a mangrove-seagrass transect in a tropical bay: Delayed groundwater seepage and seagrass uptake. *Cont Shelf Res* 172:57–67. <https://doi.org/10.1016/j.csr.2018.10.008>
- Macreadie PI, Anton A, Raven JA, Beaumont N, Connolly RM, Friess DA, Kelleway JJ, Kennedy H, Kuwae T, Lavery PS, Lovelock CE, Smale DA, Apostolaki ET, Atwood TB, Baldock J, Bianchi TS, Chmura GL, Eyre BD, Fourqurean JW, Hall-Spencer JM, Huxham M, Hendriks IE, Krause-Jensen D, Laffoley D, Luisetti T, Marbà N, Masque P, McGlathery KJ, Magonigal JP, Murdiyarto R, Santos R, Serrano O, Silliman BR, Watanabe K, Duarte CM (2019) The future of Blue Carbon science. *Nat Commun.* 10:1–13. <https://doi.org/10.1038/s41467-019-11693-w>
- Maher DT, Eyre BD (2012) Carbon budgets for three autotrophic Australian estuaries: Implications for global estimates of the coastal air-water CO<sub>2</sub> flux. *Glob Biogeochem Cycles.* <https://doi.org/10.1029/2011GB004075>
- Maher DT, Santos IR, Golsby-Smith L, Gleeson J, Eyre BD (2013) Groundwater-derived dissolved inorganic and organic carbon exports from a mangrove tidal creek: The missing mangrove carbon sink? *Limnol Oceanogr* 58(2):475–488. <https://doi.org/10.4319/lo.2013.58.2.0475>
- Maher DT, Cowley K, Santos IR, Macklin P, Eyre BD (2015) Methane and carbon dioxide dynamics in a subtropical estuary over a diel cycle: Insights from automated in situ radioactive and stable isotope measurements. *Mar Chem* 168:69–79. <https://doi.org/10.1016/j.marchem.2014.10.017>
- Maher DT, Santos IR, Schulz KG, Call M, Jacobsen GE, Sanders CJ (2017) Blue carbon oxidation revealed by

- radiogenic and stable isotopes in a mangrove system. *Geophys Res Lett.* <https://doi.org/10.1002/2017GL073753>
- Maher DT, Call M, Santos IR, Sanders CJ (2018) Beyond burial: lateral exchange is a significant atmospheric carbon sink in mangrove forests. *Biol Lett.* <https://doi.org/10.1098/rsbl.2018.0200>
- Mandal SK, Dey M, Ganguly D, Sen S, Jana TK (2009) Biogeochemical controls of arsenic occurrence and mobility in the Indian Sundarban mangrove ecosystem. *Mar Pollut Bull* 58(5):652–657. <https://doi.org/10.1016/j.marpolbul.2009.01.010>
- Mcleod E, Chmura GL, Bouillon S, Salm R, Björk M, Duarte CM, Lovelock CE, Schlesinger WH, Silliman BR (2011) A blueprint for blue carbon: toward an improved understanding of the role of vegetated coastal habitats in sequestering CO<sub>2</sub>. *Front Ecol Environ* 9(10):552–560. <https://doi.org/10.1890/110004>
- Mitra A, Gangopadhyay A, Dube A, Schmidt AC, Banerjee K (2009) Observed changes in water mass properties in the Indian Sundarbans (northwestern Bay of Bengal) during 1980–2007. *Curr Sci* 97:1445–1452
- Miyajima T, Miyajima Y, Hanba YT, Yoshii K, Koitabashi T, Wada E (1995) Determining the stable isotope ratio of total dissolved inorganic carbon in lake water by GC/C/IRMS. *Limnol Oceanogr* 40(5):994–1000. <https://doi.org/10.4319/lo.1995.40.5.0994>
- Neogi SB, Dey M, Lutful Kabir SM, Masum SJH, Kopprio GA, Yamasaki S, Lara RJ (2016) Sundarban mangroves: diversity, ecosystem services and climate change impacts. *Asian J Med Biol Res* 2(4):488–507. <https://doi.org/10.3329/ajmbr.v2i4.30988>
- Pant V, Girishkumar MS, Udaya Bhaskar TVS, Ravichandran M, Papa F, Thangaprakash VP (2015) Observed interannual variability of near-surface salinity in the Bay of Bengal. *J Geophys Res: Oceans.* <https://doi.org/10.1002/2014JC010340>
- Parsons TR, Maita Y, Lalli CM (1992) A manual of chemical and biological methods for sea water analysis. Pergamon, New York
- Pendleton L, Donato DC, Murray BC, Crooks S, Jenkins WA, Sifleet S, Craft C, Fourqurean JW, Kauffman JB, Marbà N, Magonigal P (2012) Estimating global “blue carbon” emissions from conversion and degradation of vegetated coastal ecosystems. *PLoS ONE.* <https://doi.org/10.1371/journal.pone.0043542>
- Prasad TG (2004) A comparison of mixed-layer dynamics between the Arabian Sea and Bay of Bengal: One-dimensional model results. *J Geophys Res: Oceans.* <https://doi.org/10.1029/2003JC002000>
- Rao RR, Sivakumar R (2003) Seasonal variability of sea surface salinity and salt budget of the mixed layer of the north Indian Ocean. *J Geophys Res: Oceans.* <https://doi.org/10.1029/2001JC000907>
- Ray R, Shahraki M (2016) Multiple sources driving the organic matter dynamics in two contrasting tropical mangroves. *Sci Total Environ* 571:218–227. <https://doi.org/10.1016/j.scitotenv.2016.07.157>
- Ray R, Majumder N, Das S, Chowdhury C, Jana TK (2014) Biogeochemical cycle of nitrogen in a tropical mangrove ecosystem, east coast of India. *Mar Chem* 167:33–43. <https://doi.org/10.1016/j.marchem.2014.04.007>
- Ray R, Rixen T, Baum A, Malik A, Gleixner G, Jana TK (2015) Distribution, sources and biogeochemistry of organic matter in a mangrove dominated estuarine system (Indian Sundarbans) during the pre-monsoon. *Estuar Coast Shelf Sci* 167:404–413. <https://doi.org/10.1016/j.ecss.2015.10.017>
- Ray R, Baum A, Rixen T, Gleixner G, Jana TK (2018a) Exportation of dissolved (inorganic and organic) and particulate carbon from mangroves and its implication to the carbon budget in the Indian Sundarbans. *Sci Total Environ* 621:335–547. <https://doi.org/10.1016/j.scitotenv.2017.11.225>
- Ray R, Michaud E, Aller RC, Vantrepotte V, Gleixner G, Walker R, Devesa J, Le Goff M, Morvan S, Thouzeau G (2018b) The sources and distribution of carbon (DOC, POC, DIC) in a mangrove dominated estuary (French Guiana, South America). *Biogeochemistry* 138(3):297–321. <https://doi.org/10.1007/s10533-018-0447-9>
- Raymond PA, Bauer JE, Cole JJ (2000) Atmospheric CO<sub>2</sub> evasion, dissolved inorganic carbon production, and net heterotrophy in the York River estuary. *Limnol Oceanogr* 45(8):1707–1717. <https://doi.org/10.4319/lo.2000.45.8.1707>
- Robinson C, Li L, Prommer H (2007) Tide-induced recirculation across the aquifer-ocean interface. *Water Resour Res.* <https://doi.org/10.1029/2006WR005679>
- Rosentreter JA, Maher DT, Erler DV, Murray R, Eyre BD (2018) Seasonal and temporal CO<sub>2</sub> dynamics in three tropical mangrove creeks – A revision of the global mangrove CO<sub>2</sub> emissions. *Geochim Cosmochim Acta* 222:729–745. <https://doi.org/10.1016/j.gca.2017.11.026>
- Sabine CL, Key RM, Feely RA, Greeley D (2002) Inorganic carbon in the Indian Ocean: Distribution and dissolution processes. *Global Biogeochem Cycles* 16(4):15–21. <https://doi.org/10.1029/2002GB001869>
- Sabine CL, Feely RA, Gruber N, Key RM, Lee K, Bullister JL, Wanninkhof R, Wong CSL, Wallace DW, Tilbrook B, Millero FJ, Kozyr A, Ono T, Rios AF (2004) The oceanic sink for anthropogenic CO<sub>2</sub>. *Science* 305:367–371. <https://doi.org/10.1126/science.1097403>
- Saito H, Tamura N, Kitano H, Mito A, Takahashi C, Suzuki A, Kayanne H (1995) A compact seawater pCO<sub>2</sub> measurement system with membrane equilibrator and nondispersive infrared gas analyzer. *Deep Sea Res. Part I: Oceanogr Res Pap* 42:2025–2033. [https://doi.org/10.1016/0967-0637\(95\)00090-9](https://doi.org/10.1016/0967-0637(95)00090-9)
- Saito, H., Kimoto, H., Nozaki, K., Kato, K., Negishi, A. and Kayanne, H. (1999). Comparative experiment of pCO<sub>2</sub> measuring instruments in coral reef environments. In 2nd International Symposium on CO<sub>2</sub> in the Ocean, National Institute for Environmental Studies. Tsukuba, Japan.
- Sanders CJ, Maher DT, Tait DR, Williams D, Holloway C, Sippo JZ, Santos IR (2016a) Are global mangrove carbon stocks driven by rainfall? *J Geophys Res: Biogeosci.* <https://doi.org/10.1002/2016JG003510>
- Sanders CJ, Santos IR, Maher DT, Breithaupt JL, Smoak JM, Ketterer M, Call M, Sanders L, Eyre BD (2016b) Examining <sup>239+240</sup>Pu, <sup>210</sup>Pb and historical events to determine carbon, nitrogen and phosphorus burial in mangrove sediments of Moreton Bay, Australia *J Environ Radioact*

- 151:623–629. <https://doi.org/10.1016/j.jenvrad.2015.04.018>
- Sandeep KK, Pant V, Girishkumar MS, Rao AD (2018) Impact of riverine freshwater forcing on the sea surface salinity simulations in the Indian Ocean. *J Mar Sys* 185:40–58. <https://doi.org/10.1016/j.jmarsys.2018.05.002>
- Santos IR, Eyre BD, Huettel M (2012) The driving forces of porewater and groundwater flow in permeable coastal sediments: A review. *Estuar Coast Shelf Sci* 98:1–15. <https://doi.org/10.1016/j.ecss.2011.10.024>
- Sarkar SK, Frančišković-Bilinski S, Bhattacharya A, Saha M, Bilinski H (2004) Levels of elements in the surficial estuarine sediments of the Hugli River, northeast India and their environmental implications. *Environ Int* 30(8):1089–1098. <https://doi.org/10.1016/j.envint.2004.06.005>
- Sarma VVSS, Krishna MS, Rao VD, Viswanadham R, Kumar NA, Kumari TR, Gawade L, Ghatkar S, Tari A (2012) Sources and sinks of CO<sub>2</sub> in the west coast of Bay of Bengal. *Tellus B: Chem Phys Meteorol*. <https://doi.org/10.3402/tellusb.v64i0.10961>
- Sea MA, Garcias-Bonet N, Saderne V, Duarte CM (2018) Carbon dioxide and methane fluxes at the air–sea interface of Red Sea mangroves. *Biogeosciences* 15:5365–5375. <https://doi.org/10.5194/bg-15-5365-2018>
- Sippo JZ, Maher DT, Tait DR, Holloway C, Santos IR (2016) Are mangroves drivers or buffers of coastal acidification? Insights from alkalinity and dissolved inorganic carbon export estimates across a latitudinal transect. *Glob Biogeochem Cycle*. <https://doi.org/10.1002/2015GB005324>
- Tishchenko PY, Semkin PY, Pavlova GY, Tishchenko PP, Lobanov VB, Marjash AA, Mikhailik TA, Sagalaev SG, Sergeev AF, Tibenko EY, Khodorenko ND, Chichkin RV, Shvetsova MG, Shkirnikova EM (2018) Hydrochemistry of the Tumen River Estuary, Sea of Japan. *Oceanology* 58(2):175–186. <https://doi.org/10.1134/S0001437018010149>
- Tokoro T, Hosokawa S, Miyoshi E, Tada K, Watanabe K, Montani S, Kayanne H, Kuwae T (2014) Net uptake of atmospheric CO<sub>2</sub> by coastal submerged aquatic vegetation. *Glob Change Biol* 20(6):1873–1884. <https://doi.org/10.1111/gcb.12543>
- Twilley RR, Chen RH, Hargis T (1992) Carbon sinks in mangroves and their implications to carbon budget of tropical coastal ecosystems. *Water Air Soil Pollut* 64:265–288. <https://doi.org/10.1007/BF00477106>
- Weiss R (1974) Carbon dioxide in water and seawater: the solubility of a non-ideal gas. *Mar Chem* 2(3):203–215. [https://doi.org/10.1016/0304-4203\(74\)90015-2](https://doi.org/10.1016/0304-4203(74)90015-2)
- Zablocki JA, Andersson AJ, Bates NR (2011) Diel aquatic CO<sub>2</sub> system dynamics of a Bermudian mangrove environment. *Aquat Geochem*. <https://doi.org/10.1007/s10498-011-9142-3>

**Publisher's Note** Springer Nature remains neutral with regard to jurisdictional claims in published maps and institutional affiliations.